GEOPHYSICAL RESEARCH LETTERS, VOL. 22, NO. 17, PAGES 2413-2416, SEPTEMBER 1, 1995

Near infrared imaging and spectroscopy of the SL-9 impacts from Calar Alto

T. M. Herbst,[1] D. P. Hamilton,[2] H. Böhnhardt,[3] and J. L. Ortiz-Moreno[4]

Abstract. Near infrared observations of the impacts of seven fragments of Comet Shoemaker-Levy 9 with Jupiter show that precursor flashes are ubiquitous and associated with phenomena at or near the time of atmospheric entry. The comet fragments appear to be a heterogenous group: some impacts produced anomalously bright precursors, while others were completely undetectable despite expectations based on pre–collision images. Strong CO emissions in spectra taken near maximum light point to hot molecular gas which cools within minutes. Finally, images of the disk of Jupiter in the two months after the collision show spreading of the impact structures at approximately 1.5° per day.

Introduction

This paper presents early results from the campaign of near infrared imaging and spectroscopy using the MAGIC infrared camera on the 3.5 meter Calar Alto telescope. Section 2 describes the MAGIC camera and summarizes the observing program. Section 3 discusses the lightcurves of the A, E, Q and S fragment impacts with particular emphasis on the event times. Finally, sections 4 and 5 present an overview of the spectroscopy and longer term monitoring of the planet. A companion paper by Hamilton *et al.* in this volume (hereafter Paper B) discusses the H and L impacts in detail and addresses the nature of the precursor flash phenomenon.

Observing Program

All the observations presented here and in Paper B come from the MAGIC infrared camera mounted at the f/10 Ritchey-Chrétien focus of the 3.5 meter telescope on Calar Alto. Herbst *et al.* (1993) describe the infrared camera in detail. MAGIC contains a 256×256 NICMOS3 HgCdTe array and operates in the J (1.13–1.37 μm), H (1.5–1.8 μm), and K (2.0–2.4 μm) photometric bands. The image scale was 0.322 arcsec/pixel for all measurements.

We used two custom filters from Omega Optical for most of the imaging program. A 2.3 μm (0.20 μm FWHM) was used alone, while the 1.7 μm (0.05 μm FWHM) filter needed an additional H filter in series to block a significant red leak discovered in the K band. High signal levels of daytime observations occasionally forced us to use a smaller pupil stop, reducing the telescope to f/45. The spectroscopic measurements used a direct–ruled ZnSe grism giving spectral resolution $\frac{\lambda}{\Delta\lambda} \sim 360$. This resolution and a two pixel wide slit gives complete K band coverage in a single exposure. Motorized wheels containing the filters, slits, and the grism permit rapid switching (< 1 minute) between direct–imaging and spectroscopy modes.

Impact Lightcurves

Figure 1 of this paper and figures 1 and 2 of Paper B contain lightcurves for seven of the ten impacts. The rapid brightening of the main peak saturated the MAGIC detector for all of the brighter events (H,L,Q1), and these lightcurves show the flux before and/or after maximum light only.

The lightcurves represent the integrated flux in a synthetic aperture placed on the southeastern limb of Jupiter. All measurements use the 2.3 μm CH_4 absorption filter for maximum contrast between the impact flash and the cloud deck. Darkening the planet also minimizes photometric errors introduced by sub–pixel shifts between the aperture and limb. We applied standard sky subtraction and flat fielding to all images. The vertical scales on the lightcurves assume an effective wavelength λ_{eff} for this filter of 2.276 μm, based on the 77 K spectral scan supplied by Omega Optical. We adopt an interpolated zero–point flux of F_ν=602.7 Jy at 2.276 μm (Bessel and Brett 1988). Each night, we measured a photometric standard at a similar airmass to Jupiter and interpolated the published magnitudes, using F_ν to establish the flux scale in the figures. The standard stars and interpolated 2.276 μm magnitudes were HD 129655 (6.69 mag), HD 162208 (7.10 mag), BS 5868 (3.03 mag), and 16 Cyg B (BS 7504B, 4.67 mag). We estimate an overall photometric uncertainty of 10–20%. Scattered light and variations in the exact placement of the f/45 pupil stop make the daytime measurements more uncertain.

The following paragraphs provide further information on each impact observation except for H and L, which are discussed thoroughly in Paper B.

Fragment A (16 July 20:11 UT). The precursor began sometime between frames taken at 20:11:10 and 20:11:30 UT (since this was the first impact, we opted for deeper exposures). A software glitch shortly thereafter suspended operations and prevented our measuring the shape and peak brightness of the precursor. Observations resumed four minutes later, prior to the start

[1]Max-Planck-Institut für Astronomie, Heidelberg
[2]Max-Planck-Institut für Kernphysik, Heidelberg
[3]Universitäts–Sternewarte, München
[4]Instituto de Astrofisica de Andalucia, Granada

Paper number 95GL01739
0094-8534/95/95GL-01739$03.00

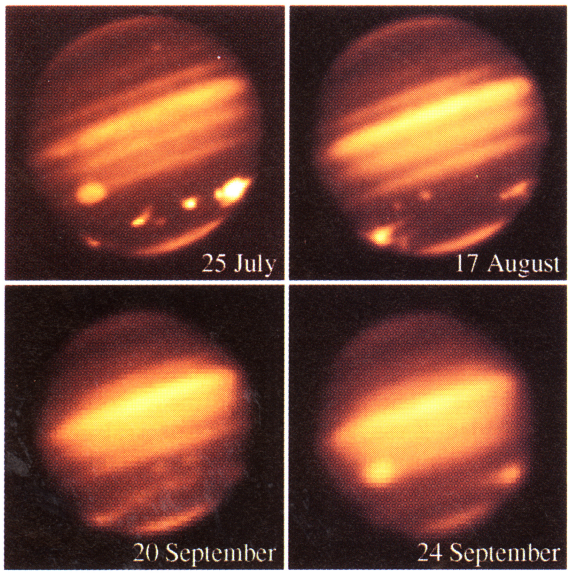

Plate 1. Aftermath of the Comet Crash. The four frames were taken in the 1.7 μm absorption band of methane on 25 July (upper left), 17 August (upper right), 20 September (lower left), and 24 September (lower right). Note that the 25 July and 24 September images show the same face of Jupiter, while the 17 August and 20 September frames show the opposite hemisphere. Significant longitudinal spreading of the impact structures took place in the months following the collision.

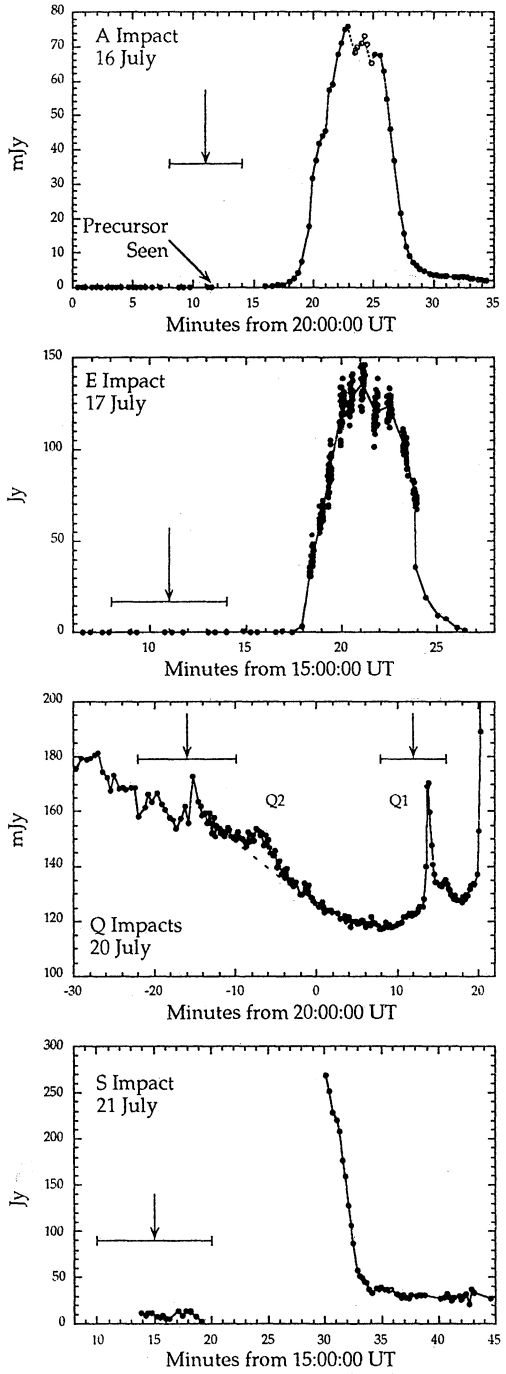

Figure 1. Lightcurves of the A, E, Q2, Q1, and S impacts. All measurements were made using the MAGIC infrared camera and the 2.3 μm filter centered on the jovian CH_4 absorption feature. The vertical arrows and horizontal error bars indicate the accepted impact times based on orbital solutions and measured impact site locations. See text for further information.

of the main peak. High flux levels drove the detector into its nonlinear range at maximum light, so the multiple peaks in figure 1 may not be real (see impact E, however). The A precursor is very evident on the original images, but was only $\sim 10^{-4}$ of the peak brightness and hence does not appear in the lightcurve in figure 1.

Fragment E (17 July 15:17 UT) The impact of fragment E was a daytime event in Spain. We rotated the f/45 cryogenic Lyot stop into place for this observation, reducing the effective telescope diameter to $\lesssim$0.5 meters. The E lightcurve, like A, shows multiple peaks which are significantly above the noise level. Also like A, the E lightcurve has a shoulder on the rising side of the main peak and a monotonically decreasing tail. The E impact had no detectable precursor, although poor seeing, reduced telescope aperture, and variations in the daytime sky level precluded sensitive measurements. We estimate any precursor was fainter than 1/2000 of the peak brightness (5 σ).

Fragments Q2, Q1 (20 July 19:44, 20:13 UT) The Q fragments struck Jupiter within half an hour of each other, and figure 1 presents a single lightcurve for both events. We observed precursors and main peaks for both impacts. The bump in the lightcurve corresponding to the main peak of Q2 appears as a distinct structure on the original images of the limb of Jupiter. The sloping baseline between 19:30 and 20:00 UT corresponds to the rotation of the pre–existing DG complex out of the synthetic aperture.

Fragment S (21 July, 15:15 UT) The S fragment impact also took place during the daytime at Calar Alto. Failure of a cooling fan caused a nine minute loss of data just before the impact, and figure 1 shows only the early and decaying phases of the lightcurve. There is no evidence of increased signal at 15:19 UT. This, combined with the shape of the A lightcurve places the onset of the main peak at 15:22±2 minutes, assuming the behaviour of the two is similar. The presence of pre-existing impact sites (L and the DG complex) and

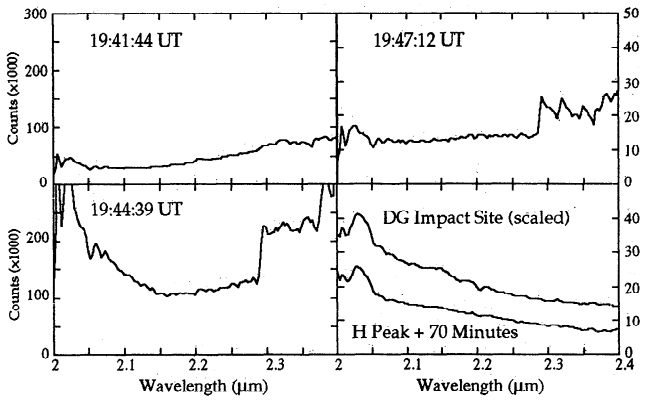

Figure 2. K band spectra of the H impact site near maximum light. The bright spectral features between 2.3 and 2.4 μm are $\Delta v = 2$ emission bandheads of CO. These lines fade within ten minutes of the peak, and after an hour, the H impact spectrum resembles that of the pre–existing DG site.

seeing and sky level variations made us insensitive to possible precursor events near 15:17 UT.

The "Lost" Impacts The P2, T and U fragment impacts occurred during clear weather with Jupiter above the horizon as seen from Spain. In all instances, we failed to detect any evidence of a precursor or main peak, although the variation in the daytime sky level coupled with poorer seeing reduced our sensitivity for the P2 and T events. The formal, 5σ upper limits on the P2 and T impact brightnesses are approximately 100 mJy, while that for the night–time U impact is approximately 1 mJy.

The primary result from the lightcurves in figure 1 (and figures 1 and 2 in Paper B) is that *all the impacts for which we have good signal to noise show distinct precursor events.* The vertical arrows on the lightcurves correspond to the accepted impact time, with the horizontal bar indicating the 1σ uncertainty. Table 1 compares these times with the onset of the precursors and the start of the main peak phase of the impact. In every instance, including those presented in Paper B, the precursor detection falls within the expected uncertainty of the accepted collision time, indicating that the precursors are associated with phenomena at or near the time of entry.

Our observations of the A impact support the tentative identification of impact phenomena in an HST image taken at 20:13:16 UT (Hammel *et al.* 1995). This image contains a few bright pixels at the expected location, but the next frame taken two minutes later shows nothing at the impact site. The impact plume appears unambiguously in a third image taken three minutes thereafter. Hammel *et al.* argue that the first frame shows the incoming bolide, while the second and third images correspond to the fragment's disappearance behind the planet and the emerging plume, respectively. The Calar Alto observations argue for a different interpretation. In Paper B, we demonstrate that two separate precursor events occur, the first apparently associated with the brief meteor flash of entry, and the second, longer–lasting one approximately a minute later corresponding to the fireball travelling up the evacuated entry channel. The first "bolide" precursor lasts for only a few tens of seconds. Our detection of the A impact at 20:11:29, almost two minutes prior to the HST image, suggests that the bright pixels in the HST frame must be associated with the second "fireball" precursor. Note that this does not require that the Calar Alto precursor correspond to the bolide, since the second precursor can last for minutes. The interruption in data–taking at 20:12 UT prevents our identification of the Calar Alto event with the first or second precursor.

The much–anticipated Q impacts on 20 July did not disappoint: figure 1 shows four distinct events within a 35 minute span. The main peak of the Q1 impact reached maximum light almost four minutes after the

Table 1. Timing Information for the 10 Impacts Visible From Calar Alto

Fragment	UT Date	Predicted Impact Time	Start of Precursor	Start of Main Event	Precursor – Main Δt	Integration time (s)
A	16 July	20:11±3	20:11:29±5	20:16:56±5	5.4 min	10,2.4
E (D)	17 July	15:11±3	nd	15:17:56±5	–	9,0.3
H	18 July	19:32±1	B	B	B	B
L	19 July	22:17±1	B	B	B	B
P2 (D)	20 July	15:23±7	nd	nd	–	4
Q2	20 July	19:44±6	19:44:47±3	19:52:24±15	7.6 min	10,0.2
Q1	20 July	20:12±4	20:13:15±3	20:19:47±3	6.5 min	10,2
S (D)	21 July	15:15±5	*	15:22±2 min†	–	4
T (D)	21 July	18:10±7	nd	nd	–	5
U	21 July	21:55±7	nd	nd	–	5,2

There is an excellent correspondence between the predicted impact time and the onset of the precursor in all instances, including the H and L impacts discussed in Paper B. We checked the absolute timing against a Global Position System (GPS) satellite receiver, as well as by measuring the disappearance of satellites behind Jupiter. All times are UT. The last column lists the various integration times used. Individual Notes: (D) – daytime observation; B – see Hamilton *et al.* in this volume (Paper B); nd – not detected; * – not detected, perhaps during gap in observations; † – estimate assumes similar behaviour to A (see text).

end of the sequence in figure 1, at which time we were monitoring the planet at 1.7 μm to avoid saturation. The Q1 precursor is remarkably similar in shape to the first "bolide" L precursor discussed in Paper B, although its duration and the 6.5 minute delay before the subsequent brightening suggests that the Q1 precursor is associated with the rising fireball and not the meteor phase. The presence of the bright DG complex and Q2 make it difficult to discern any possible bolide for Q1.

The impact of fragment Q2 was unique among the events observed in having a short–lived precursor flash of comparable brightness to the main peak itself. One possible explanation of the Q2 behaviour is that the impactor was not very solid: poor structural integrity would cause the object to "pancake" high in the atmosphere, depositing a significant fraction of its energy on entry. The delay between the observed precursor and the main peak was 1–2 minutes longer than with other impacts, matching the interval observed between the first and second precursors in H and L. Perhaps Q2 had only a first, "bolide" precursor.

There are a number of possible explanations of our nondetection of the P2 and T fragment collisions. P2 struck Jupiter between the K and C impacts at a location relatively free of pre–existing sites. Co–added images of the planet in the 1.7 and 2.3 μm CH_4 absorption bands taken at 15:40, 16:30, 17:30, and 19:00 UT show no evidence of the impact as the region rotated into view. This is somewhat surprising, since HST imagery earlier in the year showed the P2 fragment at comparable brightness to E, whose impact we easily detected during daytime. P2 was one of the more dynamic fragments in the months before impact, however, and may have not been a solid particle when it reached Jupiter. IAU Circular 5947 reported a somewhat diffuse appearance in January 1994, and two months later, IAU Circular 5973 announced that P2 had split into two distinct objects. Fragment T did not show such behaviour in the preceding months, but this object was among the faintest, and the impact occurred several hours before sunset in Spain.

The nondetection of the night–time U impact is more surprising, since we monitored the planet continuously under excellent conditions for more than an hour centered at the predicted collision time. HST images early in the year suggested that the impactor was comparable to A. Fragment U presumably struck very close to the still–bright K impact site, which was of course rising at the time. This, coupled with seeing variations, reduced our sensitivity, but we would have certainly seen an event comparable to the A impact. A similar camera on the 5 m Hale telescope also failed to detect the U impact, and no spot appeared in subsequent HST images (P.Nicholson, private communication, Hammel *et al.* 1995). These differences reinforce the notion that the fragments of Comet Shoemaker–Levy 9 were a heterogenous group.

Spectroscopy

Figure 2 shows a subset from a sequence of K band spectra centered on the main peak of the H impact. After sky–subtraction and flat–fielding, we used the positions of telluric absorption features to calibrate the wavelength scale in each extracted spectrum. Dividing the spectra by that of a G3V calibrator star (BS 7504B) then multiplying by a blackbody at the same temperature eliminates the telluric features and yields the correct spectral slope.

Deep absorption bands due to molecular hydrogen (2.12 μm) and methane (2.3 μm) darken the planet at these wavelengths. Near maximum light, prominent emission features appear longward of 2.29 μm. These arise from the $\Delta v = 2$ vibrational–rotational bandheads of carbon monoxide. CO bandhead emission is an indicator of hot molecular gas. Preliminary fits of the line profiles indicate temperatures in excess of 2000 K and significant optical depth (Herbst et al. 1995). The complete collapse of the bandhead emission within ten minutes of maximum light suggests that this hot phase is of short duration. After one hour, the spectrum of the newly–formed impact structure resembles that of pre–existing sites that are twelve hours to several days old (figure 2).

Long Term Monitoring

The images in Plate 1 show the disk of Jupiter at three epochs: 3.5 days after the final fragment impact, one month later, and two months later. The observations of 25 July and 24 September were at similar jovian Central Meridian Longitude (CML, note the Great Red Spot). The frames of 17 August and 20 September show the opposite hemisphere of Jupiter, also at approximately the same CML (note the south temperate ovals).

Considerable spreading of the impact structures took place in the months immediately after the collision, and by October, the entire southern hemisphere was girded with impact ejecta. Identifying the tendrils in Plate 1 with their parent impact sites allows an estimate of the rate of longitudinal spreading. The 17 August frame shows extended features likely associated with the K fragment on the eastern (left) side of the disk, and with the E impact on the western side. Locating the edges of these structures and deprojecting their longitude leads to a spread rate of approximately 1.2° per day, or $\sim$10 m s^{-1}. The almost complete closing of the gap between the K and A impact sites by 20 September points to a spread rate of $\lesssim$1.6° per day. The rate of latitudinal spreading is more difficult to quantify, but must be below 0.5 m s^{-1}.

References

Bessel, M. S. and Brett, J. M., JHKLM Photometry: Standard Systems, Passbands, and Intrinsic Colors, Publ. A. S. P.. 100, 1134, 1988.

Hamilton, D. P., Herbst, T. M., Böhnhardt, H.,Ortiz–Moreno, J–L,Calar Alto Observations of Shoemaker Levy 9: Characteristics of the H and L Impacts, this issue. (Paper B) 1995.

Hammel, H. B., *et al.*, Hubble Space Telescope imaging of Jupiter: Atmospheric phenomena created by the impact of comet Shoemaker-Levy 9, *Science*, 267, 1288, 1995.

Herbst, T. M., Hamilton, D. P., Böhnhardt, H.,Ortiz–Moreno, J–L, SL9 Impact Imaging, Spectroscopy, and Long–Term Monitoring from the Calar Alto Observatory, Proceedings of the European SL-9/Jupiter Workshop (R. West and H. Böhnhardt, editors), in press, 1995.

Herbst, T. M., *et al.*, MAGIC: A New Near Infrared Camera for Calar Alto, in SPIE Technical Conference 1946, p. 605, 1993.

(received December 20, 1994;
accepted June 8, 1995.) revised May 26, 1995;